Facile decoration and characterization of multi-walled carbon nanotubes with magnetic Fe_3O_4 nanoparticles

YUEDAN ZHONG[a], GUIYIN LI[b], SUQIN LIU[a*], MING ZHONG[c], HAO WANG[a], HONGLIANG LI[a]

[a]College of Chemistry and Chemical Engineering, Central South University, Changsha 410083, People's Republic of China
[b]School of Life and Environmental Sciences, Guilin University of Electronic Technology, Guilin 541014, People's Republic of China
[c]College of Chemistry and Chemical Engineering, Hunan Institute of Science and Technology, Yueyang 414006, People's Republic of China

Magnetic Fe_3O_4/multi-walled carbon nanotubes (MWNTs) nanocomposites have been fabricated by a green and simple hydrothermal method. It has been found that Fe_3O_4 nanoparticles with diameters in the range of 15-30 nm were firmly decorated on the external surfaces of MWNTs. The Fe_3O_4/MWNTs nanocomposites exhibited good ferromagnetic behavior with a high saturation magnetization of 55.833 emu/g and a coercivity of 97.062 G. Furthermore, the Fe_3O_4/MWNTs nanocomposites could be quickly separated or redispersed from aqueous solution with the application of external magnetic field.

1. Introduction

With the rapid development of nanotechnology , carbon nanotubes (CNTs), including multi-walled carbon nanoutubes (MWNTs) and single-walled carbon nanotubes (SWNTs), have attracted considerable attention for their fascinating one-dimensional tubular structures and outstanding electrical, mechanical, chemical, thermal properties [1-2]. However, the further applications of CNTs were limited due to its insolubility in any organic solvent and water [3]. In recent years, much attention has been paid to the decoration of CNTs by foreign materials in order to further improve their properties and function with the aim of extending their applications in various technology fields. In these methods, the surface modification of CNTs has been the focus of intensive study, which can not only improve their relevant properties, but also efficiently fabricate novel composites and expand their applications in heterogeneous catalysts, supercapacitors, Li-ion batteries materials, magnetic data storages and biological fields for their high surface area, low resistivity, and good chemical stability [4-5]. Among them, functionalization of CNTs with magnetic Fe_3O_4 nanoparticles has been suggested to be of great importance owing to their biocompatibility and potential applications in cancer therapy [6], magnetic fluid separation [7], contaminant treatment [8], electrochemical biosensor [9], and so on. Georgakilas et al. [10] has synthesized the Fe_3O_4 modified CNTs by non-covalent modification with pyrene as interlinker, and they found that the modified carbon nanotubes have high solubility in organic media. In fact, magnetic particles have played significant role in biomedical applications, such as drug delivery, hyperthermia agents and cell/enzyme immobilization [11]. With the help of magnetic cores, CNTs could be more potential used in biomedicine, for biological interests interacted with them can be manipulated under external magnetic fields.

Different approaches had been used to generate magnetic Fe_3O_4/CNTs nanocomposites such as chemical vapor deposition (CVD) [12], co-precipitation method [13], impregnation-pyrolysis method [14], layer-by-layer assembly technique [15], polyol method [16], and hydrothermal process [4]. Huang et al.[17] introduced carboxylic acid groups onto the walls or ends of the individual CNT/Fe_3O_4 composite nanofiber by sonication, and the carboxylated products were excellent for use in cell magnetic separation. However, most of these methods are required complicated and time-consuming operations, or need expensive raw materials. Furthermore, some of them are used organic solvents, such as benzene, methylbenzene, and hydrazine hydrate, which are toxic to humans and cause long-term harm to the environment. Therefore, a facile and effective method to prepare Fe_3O_4/CNTs nano-composites is necessary for the present situation.

In this paper, a very facile, green and efficient hydrothermal process to decorate MWNTs with Fe_3O_4 nanoparticles was reported. The hydrothermal method could be implemented with simple operation, coat-efficiency and capability for large-scale production. The obtained nanocomposites were characterized by

Fourier transform infrared spectroscopy (FTIR), scanning electron microscopy (SEM), transmission electron microscopy (TEM), X-ray powder diffraction (XRD), X-ray photoelectron spectroscopy (XPS), and vibrating sample magnetometer (VSM). Also, a possible formation mechanism of the Fe_3O_4/MWNT nanocomposites was proposed. In all, these Fe_3O_4/MWNT nanocomposites might have great applications in the immobilized enzyme system or drug delivery and many other industrial processes.

2. Material and methods

2.1. Materials

MWNTs with a purity of more than 95% and an outer diameter of 40-60 nm were provided by Shenzhen Nanotech Port Co., Ltd. Ferrous sulphates heptahydrate ($FeSO_4·7H_2O$) and aqueous ammonia solution ($NH_3·H_2O$) were purchased from Tianjin No.3 Chemical Plant. H_2O_2 and polyethylene glycol (PEG-20000) were obtained from Sinopharm Chemical Reagent Co., Ltd. Other chemicals were of analytic grade and used without further purification. All solutions were prepared with distilled, deionized water.

2.2 Pre-treatment of MWNTs with concentrated nitric acid

In order to remove the impurities, the pristine MWNTs were first suspended in concentrated nitric acid (68 %) and refluxed at 120 °C for 24h. After cooling down to room temperature, the blank solution was filtered. The obtained MWNTs were rinsed for several times until the pH value reached neutral, then dried in vacuum at 60 °C for future use.

2.3 Preparation of Fe_3O_4/MWNTs nanocomposites

The Fe_3O_4/MWNTs nanocomposites were prepared by hydrothermal method using $FeSO_4·7H_2O$ as the iron source, H_2O_2 as the oxidant and acid treated MWNTs as starting reagents. In a typical procedure, 200 mg HNO_3-treated MWNTs was first dispersed in 15 ml deionized water by sonication for 15 min. Then, 4.5 mmol $FeSO_4·7H_2O$ (1.251 g) was dissolved into the above solution and 5 ml polyethylene glycol solution (50 g·L^{-1}) was added. The solution was achieved at 30℃ under vigorous stirring by adding 15 ml of diluted ammonia (2.5%) was added. During the reaction process, the pH was maintained at about 10. Afterwards, 0.135 ml 30% H_2O_2 was added slowly into the solution and the reaction mixture was stirred for 10 min to obtain a homogeneous solution. After that, the as-formed slurry was transferred into a 50 ml Teflon-lined stainless steel autoclave and was heated at 160 °C for 5 h in a furnace.

After cooling down to the room temperature, the Fe_3O_4/MWNTs nanocomposites were recovered from the reaction mixture by a permanent magnet with a surface magnetization of 6000 G, and washed three times with water and ethanol, dried at 80 °C for 12 h under vacuum.

2.4. Characterization of Fe_3O_4/MWNTs nanocomposites

FTIR spectra of the treated MWNTs and the Fe_3O_4/MWNT nanocomposites were recorded with KBr discs in the range of 4000-400cm^{-1} on Nicolet 560 Fourier-transfer infrared spectroscopy. The average particle size, size distribution and morphology of Fe_3O_4/MWNTs nanocomposites were studied by SEM (JEM-6360LV), TEM and HRTEM (HRTEM, JEM-2100F). The crystallographic information of the samples was investigated using X-ray powder diffraction (Japan D/max2550 X-ray diffractometer) with Cu Kα irradiation at λ=1.54178Å with 4^0 min^{-1} scan rate. A continuous scan mode was used to collect 2θ data from 10°-80°. XPS analyses were performed by a K-Alpha 1063 electron spectrometer from Thermo Fisher. Magnetic measurements were carried out with a vibrating sample magnetometer (Lake Shore 7410) at room temperature.

3. Results and discussion

3.1 The formation of Fe_3O_4/MWNTs nanocomposites

The Fe_3O_4/MWNTs nanocomposites were prepared by hydrothermal method using $FeSO_4·7H_2O$ as the iron source, H_2O_2 as the oxidant and acid treated MWNTs as starting reagents. It is well-known that treating the CNTs with nitric acid could create considerable functional groups such as carboxyl on the out surface of CNTs which become negatively charged. The positive metal ions in the system would attach to and interact with the carboxylic groups via electrostatic attraction and serve as nucleation precursors (Fig. 1). As the acid treatment proceeds, continuous attack at the defects would enlarge those damages along CNTs and eventually cut the nanotubes, in which not only the amount of COOH groups is increased but also the COOH groups that used to be on the sidewall are now on the new open ends of shortened nanotubes. After oxidation by concentrated HNO_3, hydroxyl groups and carbonyl groups are formed on the MWNTs surfaces, which make the treated MWNTs disperse easily in water in a stable manner. It is obvious that such negatively charged functional groups on the MWNTs surfaces can absorb positive charge Fe^{2+} species through electrostatic attraction, which may act as the nucleation center. After the addition of the $NH_3·H_2O$, these metal ions in situ react with OH^-, and $Fe(OH)_2$ precipitates are formed as coatings on the MWNTs surface. In the following hydrothermal process, Fe_3O_4 crystallites are produced by

oxidizing the Fe(OH)$_2$ precipitates. These nuclei could initiate the growth of Fe$_3$O$_4$ nanoparticles, and then attach tightly to nanotube surfaces, resulting in Fe$_3$O$_4$/MWNTs nanocomposites. This reaction can be expressed as
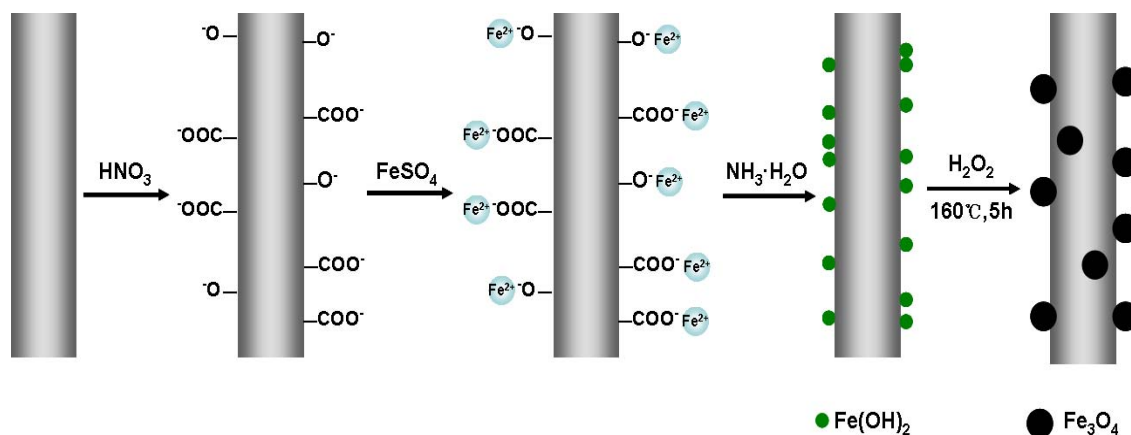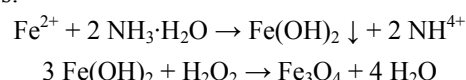
follows:

$$Fe^{2+} + 2\ NH_3 \cdot H_2O \rightarrow Fe(OH)_2 \downarrow + 2\ NH^{4+}$$

$$3\ Fe(OH)_2 + H_2O_2 \rightarrow Fe_3O_4 + 4\ H_2O$$

Fig. 1. Schematic illustration of the decoration of MWNTs with Fe₃O₄ nanoparticles in the hydrothermal system.

Generally, the main driving force for oriented aggregation of Fe$_3$O$_4$ nanocrystals into nanoparticles is attributed to the tendency to decrease the high surface energy [18]. In our case, dipolar interactions between the magnetite nanocrystals are also contributive to their aggregation. Moreover, the agent PEG-20000 could prevent fast growth of Fe$_3$O$_4$ crystallite due to a better steric effect and hinder self-aggregation of Fe$_3$O$_4$ nanoparticles , which can further reduce the size of Fe$_3$O$_4$ aggregation [18,19]. The retained interaction between Fe$_3$O$_4$ nanoparticles and MWNTs may be both electrostatic interation and van der waals force.

3.2. FTIR spectra analysis

The pristine MWNTs in our experiments were first treated by oxidation process using concentrated HNO$_3$. FT-IR spectra studies of the treated MWNTs and Fe$_3$O$_4$/MWNTs nanocomposites (Fig. 2) indicated that the acid-treatment generated three types of functional groups on the MWNT surfaces: hydroxyl groups (3433.12 cm⁻¹), carbonyl groups (1638.70 cm⁻¹), and C-O stretching band (1070.66 cm⁻¹) [20]. Due to these hydrophilic groups, the treated MWNTs could be easily dispersed in aqueous solvent, and form stable suspensions without visible aggregation even after two months (see Fig. 3). This mild functionalization is an effective method in preparing water-soluble MWNTs. Compared to the treated MWNTs (Fig. 2a), a peak at 578.67 cm⁻¹ for the composites (Fig. 2b) can be seen, which is the stretching vibration due to the interactions of Fe-O-Fe in Fe$_3$O$_4$ (magnetite), similar to the results in the literatures [21, 22].
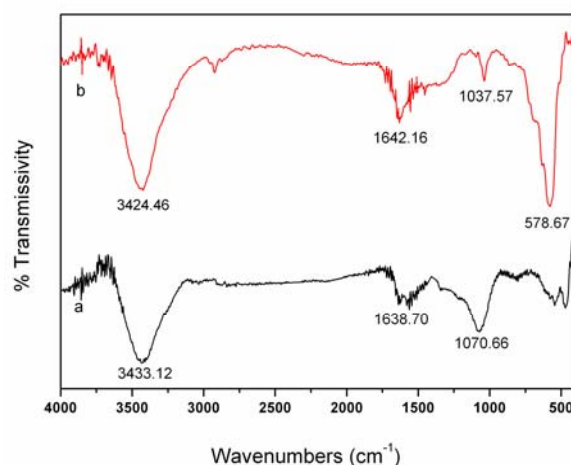

Fig. 2. FTIR spectra of treated MWNTs (a) and Fe₃O₄/MWNTs nanocomposites (b).

Fig. 3. The water-solubility of pristine MWNTs and treated MWNTs.

3.3 SEM images of Fe$_3$O$_4$/MWNTs nanocomposites

Fig. 4 illustrated the typical SEM images of pristine MWNTs, treated MWNTs, and Fe$_3$O$_4$/MWNTs composites. The pristine MWNTs in our experiments were first treated by oxidation process using concentrated HNO$_3$. According to previous reports [19,23], the mixed oxidizing acids or concentrated HNO$_3$ have been often applied as an effective method in opening the ends of CNTs as well as cutting CNTs through destroying their defect sites preferentially. The pristine MWNTs (Fig. 4a) represent the highly entangled morphology and amorphous impurities. After purification process using concentrated HNO$_3$, the treated MWNTs (Fig. 4b) indicate the obvious reduction of amorphous nanoparticles and bundled MWNTs. Moreover, it can be seen that the average length of MWNTs has reduced several micrometers of nanometers after acid treatment. Fig. 4c gives the representative SEM image of the products, which indicates that the external surfaces of MWNTs are densely deposited with Fe$_3$O$_4$ nanoparticles.
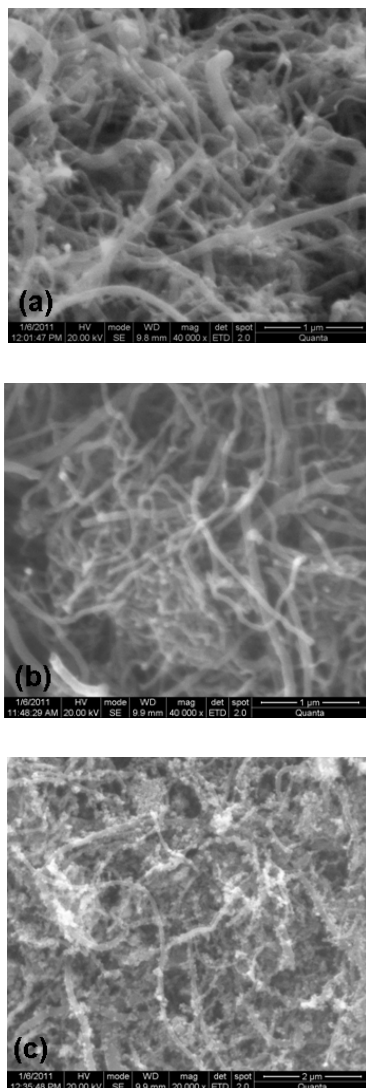
3.4 TEM images of Fe$_3$O$_4$/MWNTs nanocomposites

The microstructure and morphology of the obtained products were investigated by TEM. Fig. 5a showed the TEM image taken from an individual hybrid structure. It is found that the Fe$_3$O$_4$ nanoparticles with diameters ranging from 15 nm to 30 nm, which is consistent with the result calculated using the Scherrer's equation, are preferentially adhered to the surfaces of MWNTs. Although the products have been sonicated in ethanol before TEM measurements, the Fe$_3$O$_4$ nanoparticles are still stably attached to the nanotube surfaces and this indicates the strong interaction between them. It has been observed that the agglomeration of Fe$_3$O$_4$ nanoparticles is adequately prevented by the deposition of Fe$_3$O$_4$ nanoparticles on MWNTs, which is consistent with the results of SEM investigation. More detailed structural information of magnetite nanoparticles and MWNTs is provided by the HRTEM analysis. The typical shape of some magnetite nanoparticles looks like cubes with a visible lattice, implying the high crystallinity of these Fe$_3$O$_4$ nanoparticles, as demonstrated in the inset of Fig. 5a. The HRTEM examination (Fig. 5b) shows that the parallel lattice fringe of 0.25 nm of an individual nanoparticle, which is close to that of the (311) lattice planes of magnetite.
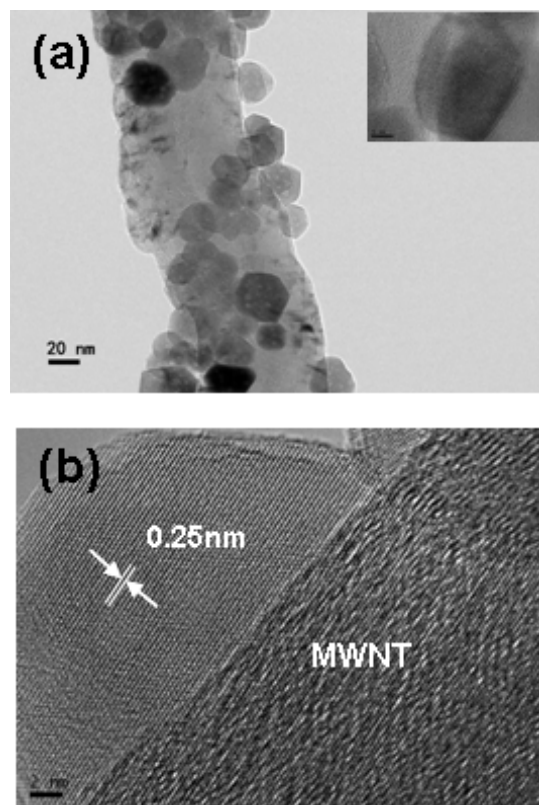

Fig. 4. SEM images of pristine MWNTs (a), treated MWNTs (b), and Fe$_3$O$_4$/MWNTs nanocomposites (c), the bar is 40000×, 40000×, and 20000×, respectively.

Fig. 5. TEM (a) and HRTEM (b) images of Fe$_3$O$_4$/MWNTs nanocomposites. The single Fe$_3$O$_4$ nanoparticle is shown in the inset of (a).

3.5 XRD analysis of Fe$_3$O$_4$/MWNTs nanocomposites

The XRD patterns of the treated MWNTs (a) and Fe$_3$O$_4$/MWNTs nanocomposites synthesized by hydrothermal process (b) are shown in Fig. 6. The analysis result indicated that the product was a mixture of two phases: cubic Fe$_3$O$_4$ (JCPDS card 88-0866) and MWNTs. The diffraction peak in Fig. 6a at 2θ=26.2° can be indexed to the (002) reflection of the MWNTs [5]. No obvious peaks from other phases are observed. In Fig. 6b, the characteristic peak of MWNTs is still exists, and all other diffraction peaks match well with the (111), (220), (311), (222), (400), (422), (511), (440), (620), (533) reflection of the magnetic cubic structure of Fe$_3$O$_4$. The strong and sharp diffraction peaks reveal the well crystallinity of the products. The average crystallite size of the Fe$_3$O$_4$ particle, calculated by Scherrer's formula, is about 21.51 nm.
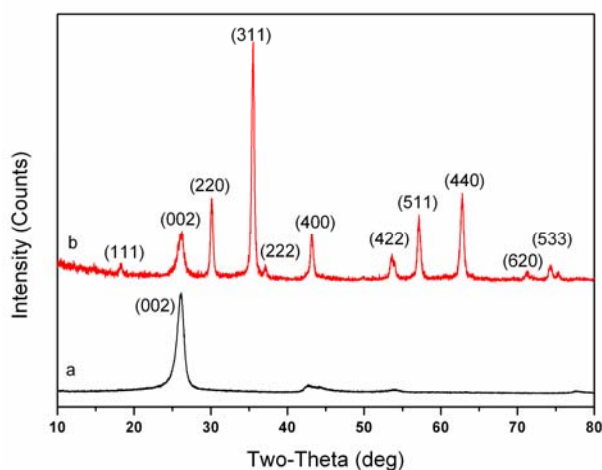

Fig. 6. XRD patterns of treated MWNTs (a) and Fe$_3$O$_4$/MWNTs nanocomposites (b).

3.6 XPS analysis of Fe$_3$O$_4$/MWNTs nanocomposites

The surface chemistry of the Fe$_3$O$_4$/MWNTs nanocomposites was investigated using XPS. Fig. 7 shows the survey scan spectra and Fe 2p narrow scan spectra for the Fe$_3$O$_4$/MWNTs composites. The strong peak of C 1s peak at 284.61 eV corresponds to carbon nanotubes, and the signals of the Fe 2p, Fe 3p, and O 1s are observed in Fig. 7. The high resolution Fe 2p spectrum (see the insert of Fig. 7) shows that the binding energies of the Fe 2p$_{3/2}$ and Fe 2p$_{1/2}$ locates at 711.08 eV and 724.78 eV, respectively, which further confirms that the oxide in the sample is Fe$_3$O$_4$ [22, 24]. The weight gain of Fe$_3$O$_4$ nanoparticles is 60.97 wt% based on the ratio of the peak areas and relative sensitivity factor.
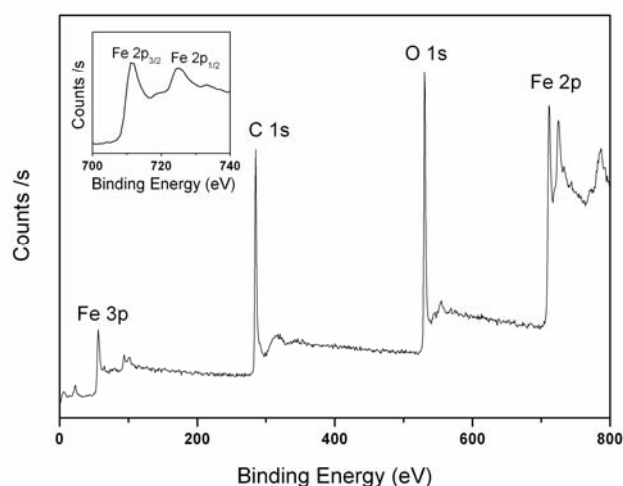

Fig. 7. XPS spectra for Fe$_3$O$_4$/MWNTs nanocomposites (the insert shows the high resolution scan of Fe 2p region).

3.7 Magnetic properties of Fe$_3$O$_4$/MWNTs nanocomposites

Further investigation on the magnetic properties of the Fe$_3$O$_4$/MWNTs nanocomposites was recorded in a vibrating sample magnetometer. Fig. 8 illustrates the room-temperature magnetization curve for the Fe$_3$O$_4$/MWNTs sample, indicating that the nanocomposites exhibit ferromagnetic behavior. The curve shows that the products have saturation magnetization of 55.833 emu/g, which is comparatively lower than that of the pure Fe$_3$O$_4$ (92 emu/g) [25] resulting from the existence of MWNTs. Correspondingly, the coercive force (Hc) of the magnetic nanocomposites as shown in the inset of Fig. 8a is 97.062 G. Magnetic separability of the sample was also tested in aqueous solution by placing a magnet near the glass bottle. The black power was attracted toward the magnet in a short period (Fig. 8b), demonstrating high magnetic sensitivity. This showed that Fe$_3$O$_4$/MWNTs nanocomposites could be easily and reliably manipulated through the application of a magnetic field. The magnetic property of the nanocomposites is important for their applications such as in catalysis, electronic devices, sensors and magnetic purpose, which needs to be further explored.
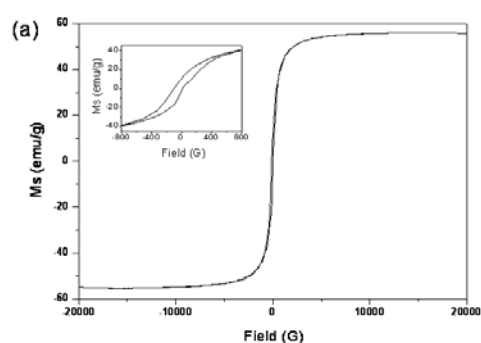
Fig. 8. Hysteresis loops of the Fe_3O_4/MWNTs nanocomposites measured at RT (a) and separation Fe_3O_4/MWNTs nanocomposites from solution under an external magnetic field (b).

4. Conclusion

In summary, a facile, efficient, one-step hydrothermal approach was developed to successfully synthesize novel Fe_3O_4/MWNTs nanocomposites, in which tiny nanocrystallites with diameters ranging from 15 nm to 30 nm were decorated exclusively on the surfaces of acid treated MWNTs, and the aggregation of magnetic nanoparticles was avoided. The saturated magnetization of nanocomposites could reach 55.833 emu/g and the nanoparticles showed the characteristics of superparamagnetism. The obtained Fe_3O_4/MWNTs nanocomposites could be readily dispersed in aqueous media and showed a high magnetic responsivity to external magnetic field. This synthesis method can be extended for depositing other metals, alloys or oxides nanoparticles onto MWNTs using appropriate precursors, displaying great potential in organization of CNT-based structures in to integrated functional devices.

References

[1] J. N. Coleman, U. Khan, Y. K. Gun'ko, Advanced Materials **18**, 689 (2006).
[2] R. H. Baughman, A. A. Zakhidov, W. A. de Heer, Science **297**, 787 (2002).
[3] M. M. J. Treacy, T. W. Ebbesen, J. M. Gibson, Nature **381**, 678 (1996).
[4] Y. Shan, K. Z. Chen, X. G. Yu, L. A. Gao, Appl. Surf. Sci. **257**, 362 (2010).
[5] L. Zhang, Q. Q. Ni, T. Natsuki, Y. Q. Fu, Appl. Surf. Sci. **255**, 8676 (2009).
[6] D. Yang, F. Yang, J. H. Hu, Chem. Commun. 4447 (2009).
[7] A. Kunkul, A. Ekmekyapar, C. Akmil, T. Abbasov, Ind. Eng. Chem. Res. **43**, 161 (2004).
[8] P. Xu, D. X. Cui, B. F. Pan, F. Gao, R. He, Q. Li, T. Huang, C. C. Bao, H. Yang, Appl. Surf. Sci. **254**, 5236 (2008).
[9] C. Gao, W. W. Li, H. Morimoto, Y. Nagaoka, T. Maekawa, J. Phys. Chem. B **110**, 7213 (2006).
[10] V. Georgakilas, V. Tzitzios, D. Gournis, D. Petridis, Chem. Mater. **17**, 1613 (2005).
[11] G. Y. Li, Z. D. Zhou, Y. J. Li, K. L. Huang, M. Zhong, Journal of Magnetism and Magnetic Materials **32**, 3862 (2010).
[12] K. Zhang, M. M. F. Yuen, J. H. Gao, B. Xu, Cirp. Ann-Manuf. Techn. **56**, 245 (2007).
[13] S. Wang, H. Bao, P. Yang, G. Chen, Analytica Chimica Acta **612**, 182 (2008).
[14] X. B. Fan, F. Y. Tan, G. L. Zhang, F. B. Zhang, Mat. Sci. Eng. a-Struct. **454**, 37 (2007).
[15] M. A. Correa-Duarte, M. Grzelczak, J. Phys. Chem. B **109**, 19060 (2005).
[16] J. Q. Wan, W. Cai, J. T. Feng, X. X. Meng, E. Z. Liu, J. Mater. Chem. **17**, 1188 (2007).
[17] Z. Huang, J. Li, Q. W. Chen, H. Wang, Mater. Chem. Phys. **114**, 33 (2009).
[18] B. P. Jia, L. Gao, J. Phys. Chem. B **11**, 5337 (2007).
[19] B. P. Jia, L. Gao, J. Gun, Carbon **45**, 1476 (2007).
[20] K. Y. Jiang, A. Eitan, L. S. Schadler, P. M. Ajayan, R. W. Siegel, NANO Letters **3**, 275 (2003).
[21] D. Shi, J. P. Cheng, F. Liu, X. B. Zhang, Journal of Alloys and Compounds 502, 365 (2010).
[22] Y. Sahoo, J. Phys. Chem. B **109**, 3879 (2005).
[23] X. Z. Wang, Z. B. Zhao, J. Y. Qu, Z. Y. Wang, J. S. Qiu, Journal of Physics and Chemistry of Solids **71**, 673 (2010).
[24] Z. Qian, Z. C. Zhang, Y. Chen, Journal of Colloid and Interface Science **327** , 354 (2008).
[25] D. H. Han, Journal of Magnetism and Magnetic Materials **136**, 176 (1994).

*Corresponding author: sqliu2003@126.com